METAL SURFACE TEXTURE CLASSIFICATION WITH GABOR FILTER BANKS AND XAI

DEMIRCIOGLU, P., SECKIN, A.C.,
TORGERSEN, J., BOGREKCI, I. & DURAKBASA, M.N.

Abstract: *This chapter introduces a novel approach for recognizing metal surfaces processed through various operations such as milling, turning, and grinding. The approach involves feature extraction using Gabor filter banks and the utilization of machine learning techniques to facilitate surface recognition. Furthermore, to enhance the interpretability of the model, Explainable Artificial Intelligence (XAI) principles are applied. This is achieved by calculating SHAP (SHapley Additive exPlanations) values for each extracted feature, shedding light on the decision-making process and improving the system's trustworthiness. The Gabor filter with a theta value of 0.79 radians (45°), sigma 5, and lambda value of 0.5 consistently emerged as the most influential feature across all classes. The results of testing on both the train and test data demonstrate a high accuracy and precision for the machine learning model.*

Key words: *Feature extraction, Gabor filter banks, Image processing, Explainable artificial intelligence.*

Authors´ data: Prof. Dr. **Demircioglu**, P[inar]*,**; Assoc. Prof. Dr. **Seckin**, A[hmet C.]*; Prof. Dr. **Torgersen**, J[an]**, Prof. Dr. **Bogrekci**, I[smail]*; Prof. Dr. **Durakbasa**, N[uman M.]***; *Aydin Adnan Menderes University, Aydin, Turkey **Technical University of Munich (TUM), TUM School of Engineering and Design, Institute of Materials Science, Germany, ***TU Wien (Vienna University of Technology), A-1060, Vienna, Austria, numan.durakbasa@tuwien.ac.at

This Publication has to be referred as: Demircioglu, P[inar]; Seckin, A[hmet]; Torgersen, J[an]; Bogrekci, I[smail] & Durakbasa, N[uman] (2023). Metal Surface Texture Classification with Gabor Filter Banks and Xai, Chapter 03 in DAAAM International Scientific Book 2023, pp.033-050, B. Katalinic (Ed.), Published by DAAAM International, ISBN 978-3-902734-39-6, ISSN 1726-9687, Vienna, Austria
DOI: 10.2507/daaam.scibook.2023.03

1. Introduction

1.1. Background for Surface Texture Detection for Machining

In today's industrial landscape, ensuring the quality of manufactured products is of great importance to meet the ever-increasing demands of consumers and comply with stringent regulatory requirements. Among the crucial quality control challenges faced by industries, the detection and classification of surface texture plays a vital role in maintaining the integrity and reliability of various components and products. The primary objective of surface texture inspection is to automatically detect, localize, and classify texture on different materials, such as metal, plastic, glass, textiles, and more. These surface textures can range from rough and irregular patterns to smooth and uniform surfaces, and they play a crucial role in determining the mechanical, physical, and aesthetic properties of the manufactured components.

Accurate and reliable surface texture detection is vital for ensuring consistent product quality, proper functionality, and compliance with industry standards and regulations. The combination of Gabor filter banks, Machine Learning and Explainable Artificial Intelligence (XAI) techniques not only improves detection performance but also provides valuable insights into the features influencing classification decisions. By harnessing this knowledge, engineers and manufacturers gain the capability to optimize processes, make well-informed design choices, and effectively address any potential challenges.

Gabor filter banks are used for texture classification in computer vision and its applications (scikit-image, 2022). They are defined by their parameters including frequencies, orientations, frequency ratio and smooth parameters (Pakdel & Tajeripour, 2011). Gabor filters have been utilized in image processing applications, especially for texture classification (Wang et al., 2019). Gabor filter banks offer a powerful approach for accurate and efficient surface texture analysis, providing manufacturers with valuable insights into product quality, process optimization, and overall customer satisfaction.

1.2. Literature for Surface Texture Classification

Surface texture detection for focusing is a fundamental aspect of modern manufacturing processes that focuses on analyzing and characterizing the surface properties of machined components. The surface texture of a manufactured product plays a crucial role in determining its quality, functionality, and performance. It encompasses various attributes such as roughness, waviness, and lay, which are essential for product functionality, aesthetics, and durability. Over the years, researchers and engineers have extensively developed methodologies and algorithms for surface texture detection. By reviewing this literature, a comprehensive understanding of the state-of-the-art in surface texture detection and its vital role in inspection processes is explained.

The classification of surface textures using various modelling approaches is discussed (Aggarwal & Kumar, 2020). The study proposes a deep learning-based model using convolution neural network (CNN) which is divided into two sub models knowing model-1 and model-2. The approach is designed with customized parameters configuration to classify surface texture using a smaller number of training samples.

The image feature vectors are generated using statistical operations to compute the physical appearance of the surface and a CNN model is used to classify the generated surfaces with appropriate labels into classes.

Sensor systems, which were previously mechanical and electrical based, have evolved into electronic and software-based systems over time. Today, the image processing technique used as a test system is becoming widespread and its importance is increasing. The process that was done with more than one sensor or system in old quality control and test systems has now become very efficient thanks to a camera and software.

The data processed in machine vision systems comprises a matrix, obtained through the emission of light and the capture of photons from objects. The lens in front of the camera collects emitted photons, directing them onto the image sensor, which places these incoming photons as values within the matrix based on their angles. Each pixel in the sensor is assigned a corresponding electrical energy value, resulting in the digitization of the image. Such images can be obtained in various forms, including x-ray, ultrasound, and thermal images, through different techniques that ultimately convert the data into digital representations.

Integrating image inspection with surface quality assessment has become essential to effectively address the significance of this parameter in the manufacturing process. This combined approach enables early detection of defects, irregularities, and deviations, ensuring that the final product meets stringent quality standards. By adopting proactive measures, manufacturers can enhance process control, minimize production errors, and deliver products that fulfill the highest quality requirements. This, in turn, fosters customer satisfaction and sustains a competitive edge in the industry (Bogrekci & Demircioglu, 2017).

Roughness measurement is a crucial aspect of assessing surface quality in diverse manufacturing processes. Compared to traditional stylus-based measurements, machine vision-based surface roughness assessments have the ability to perform at higher speed without scratching the surface, detect submicron measurements due to the geometry of mechanical tips, and monitor cone-like irregularities. In addition, machine vision methods have a more consistent evaluation ability than mechanical (manual) examination methods.

According to standard ISO 8688 (ISO 8688, 2016), surface topography can be characterized by geometric parameters, such as Ra (average of the independent measurements of a surface's peaks and valleys) and Rmax (maximum height roughness). According to the ISO 4287 standard (ISO 4287, 2021), the parameter Ra is the is the most frequently used surface parameter in the fastest surface topography evaluations in surface quality evaluations in the industry.

Ra quantifies the average height variations over a surface, with higher values indicating rougher textures and lower values indicating smoother textures. Ra is crucial in manufacturing processes for quality control, ensuring that machined components meet desired specifications. It serves as a key metric to assess surface texture suitability for specific applications. In surface texture detection algorithms, Ra is often utilized as an input parameter, enabling automated quality assessment and defect detection through image processing and statistical techniques. An automatic inspection system and its design to be used in the detection of surface defects such as scratches and potholes on the automobile surface are presented in (Chen et al., 2019).

First, the problem of unbalanced lighting is discussed for a more accurate determination. This problem has been solved by creating a contactless image acquisition device with four LED (Light Emitting Diode) light sources in a closed environment. From the image of these defective regions using CCD camera, a classification of defects as pits and scratches was trained a support vector machine algorithm. Experimental results showed that the automatic inspection system achieves 95.6% accuracy for pit defects and 97.1% accuracy for scratch defects.

A real-time defect detection approach using a Support Vector Machine (SVM) to reduce product damage and production cost in machined steel is presented in (Chang et al., 2004). With this approach, defects in steel have been examined and a system that automatically learns decision limits when data noise occurs. SVM learning algorithm has been developed. It has been shown by experimental results that the algorithm detects the error in real-time application.

A system that can monitor the defects in the casting extrusion manufacturing process in real time and uses the refraction of a collimated light source called Mie light scattering is proposed in the study in (Gamage & Xie, 2008). A vision analysis system with a drop analysis is used to detect contrasting dark areas of flaws. Flaw detection system can detect the number, type, size and location of defects. In the test results, it has been shown that the proposed system in the hardware created for the test gives high accuracy results.

The study by Cai et al. (2010) proposes a machine vision-based automatic detection system for identifying bearing surface defects. It uses least squares fitting and ring scanning to locate detected regions in the bed. The system converts annular images into rectangular images using polar cartesian coordinate transformation to facilitate error detection. Size filtering is applied to exclude regions without defects, and circularity is used to classify defects. In simulated results using the LabVIEW program, the system achieved a detection accuracy of 92% for defects.

With the aid of XAI techniques like SHAP plots, researchers can gain a deeper understanding of complex machine learning models, making them more transparent and trustworthy. This transparency not only improves model interpretability but also helps in identifying potential biases and ensuring fair and ethical deployment of AI algorithms in various applications. As XAI continues to evolve, it is expected to play an increasingly significant role in promoting accountability and reliability in AI systems (Seckin & Seckin, 2022; Sabry et al., 2023; Shuai et al., 2022).

2. Previous Works

In modern manufacturing, achieving the right surface finish is crucial to meet product performance criteria, optimize functionality, and enhance the overall appearance for end-users. In our previous work, experiments using specimens manufactured through various machining processes, such as surface grinding, front milling, and face turning were conducted. Figure 1 displays images of surfaces with three different roughness values: 0.498μm, 2.382μm, and 3.984μm (Ra), each computed as the average of ten consecutive measurement values taken. These roughness values provide essential insights into the surface quality of the specimens, aiding in quality control and optimization in manufacturing processes.

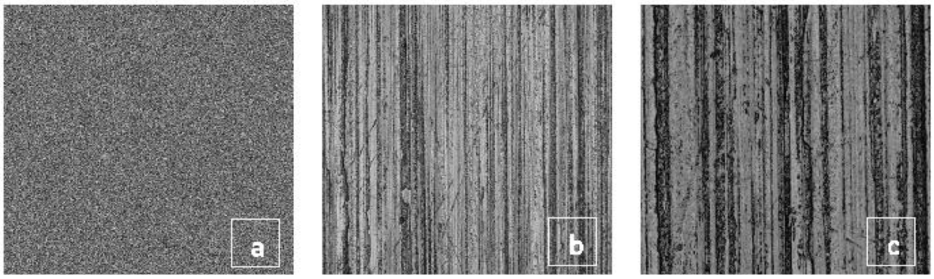

Fig. 1. The images taken from the workpieces a) Ground surface (Ra=0.498µm), b) Front Milled surface (Ra=2.382µm) and c) Face Turned surface (Ra=3.984µm) (Bogrekci & Demircioglu, 2017; Demircioglu et al., 2013)

The images of three samples with three different surface roughness values were trained in various algorithms such as Fast Fourier Transform (FFT), Wavelet Transform, Line Scanning and Speckle Infusion. 2D FFT algorithms convert the spatial domain image to the frequency domain image. 8-bit gray-level images were obtained from captured color images. An eight-bit gray image was binarized using different threshold levels. Binary images are analyzed using FFT. Percentages of black and white pixel counts of the converted images are then calculated for verification. Figure 2 exhibited that the number of black pixels in the image increased with surface roughness values.

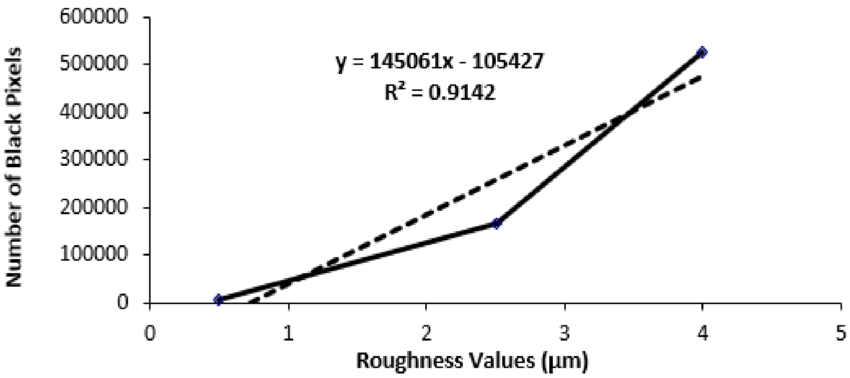

Fig. 2. The number of Black (Dark) pixels from FFT images taken from images of workpieces a) Ground surface (Ra = 0.498µm), b) Front Milled surface (Ra = 2.382µm) and c) Face Turned surface (Ra = 3.984µm) (Bogrekci & Demircioglu, 2017; Demircioglu et al., 2013)

True color images were first converted into binarized digital number (DN) values. Binarization is a process that converts grayscale or color images into binary images. Using the binarized images, the researchers applied LS technique to collect DN values from selected lines in the images. LS involves analyzing specific lines or regions of interest in the images to extract relevant data. From these analyses, pulse widths of signals confirmed that pulse widths increased with increase in surface roughness. The results of LS from Figures 3a, 3b and 3c clearly indicate that pulse numbers are different for each surface. The number of pulses is 28, 11 and 5 respectively for ground, front milled and face turned surfaces. Also pulse widths of signals confirm that pulse widths increase with increase in surface roughness.

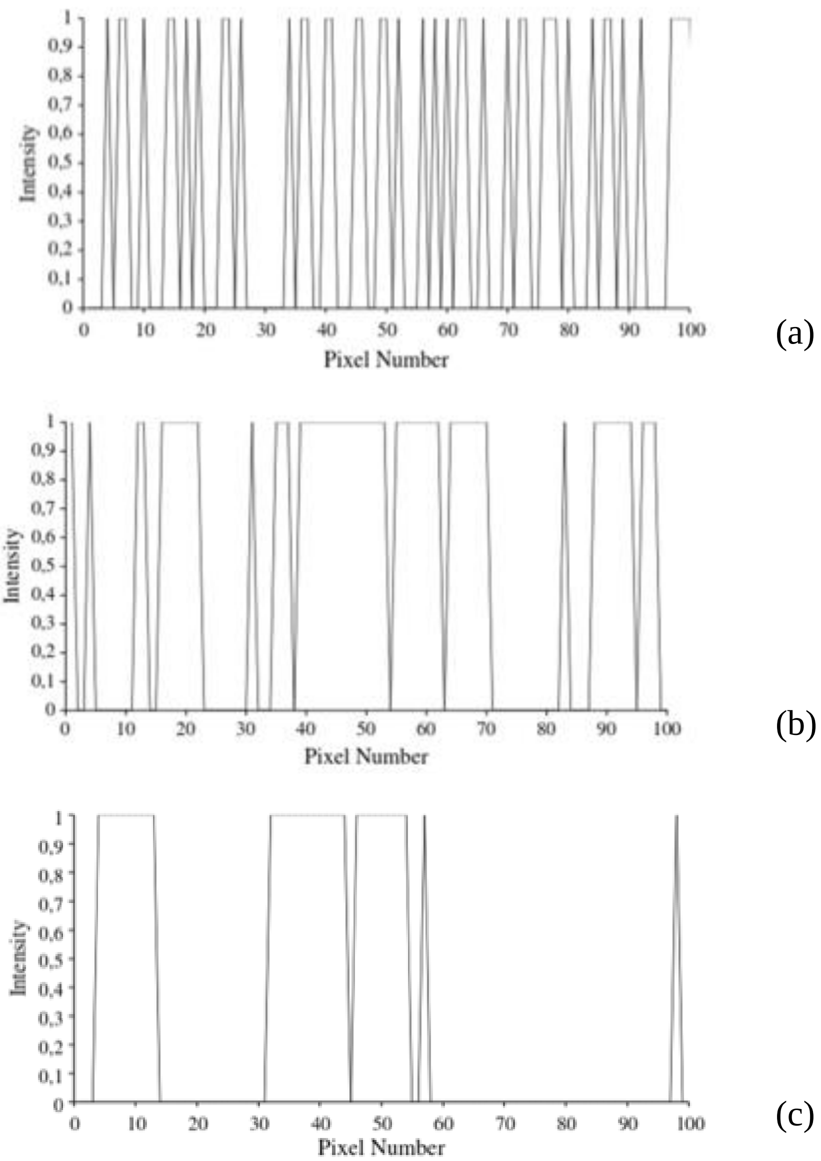

Fig. 3. The signal taken from the image with a) Ground surface (Ra = 0.498μm), b) Front Milled surface (Ra = 2.382μm) and c) Face Turned surface (Ra = 3.984μm) (Bogrekci & Demircioglu, 2017; Demircioglu et al., 2013)

Wavelet Transform (WT) functions (Teolis, 1998) as decomposing the image into its frequencies but preserving the information coming from spatial domain. Decomposition can be explained as the application of filtering. pass filters). The images were decomposed into frequencies by WT. Decomposition was performed by applying filtering low-and high-pass filters. It helps in understanding the different frequency characteristics of the image and can be used for various applications, such as feature extraction and texture analysis.

When a rough surface is imaged with the laser beam, a subjective speckle pattern is formed on the image plane. The speckle pattern was used for estimation of roughness values in our previous studies. Speckle analyses results clearly specified that as the roughness enlarged both sharpness and color distinctions increased (Bogrekci & Demircioglu, 2017; Demircioglu et al., 2013).

3. Material and Method

Grinding, milling, and turning are three common machining processes having its characteristics and effects on surface texture, which play a crucial role in determining the quality and functionality of the final product. Grinding typically produces a fine and uniform surface texture with low roughness values. Milling is commonly used for shaping and contouring surfaces. Turning is widely used for cylindrical components and creating rotational symmetry (Neslihan et al., 2022).

The main method used in the study is shown as a flowchart in Figure 4. the study utilized image capturing, feature extraction using Gabor filter bank, data splitting, model training, and SHAP (SHapley Additive exPlanations) for model interpretability.

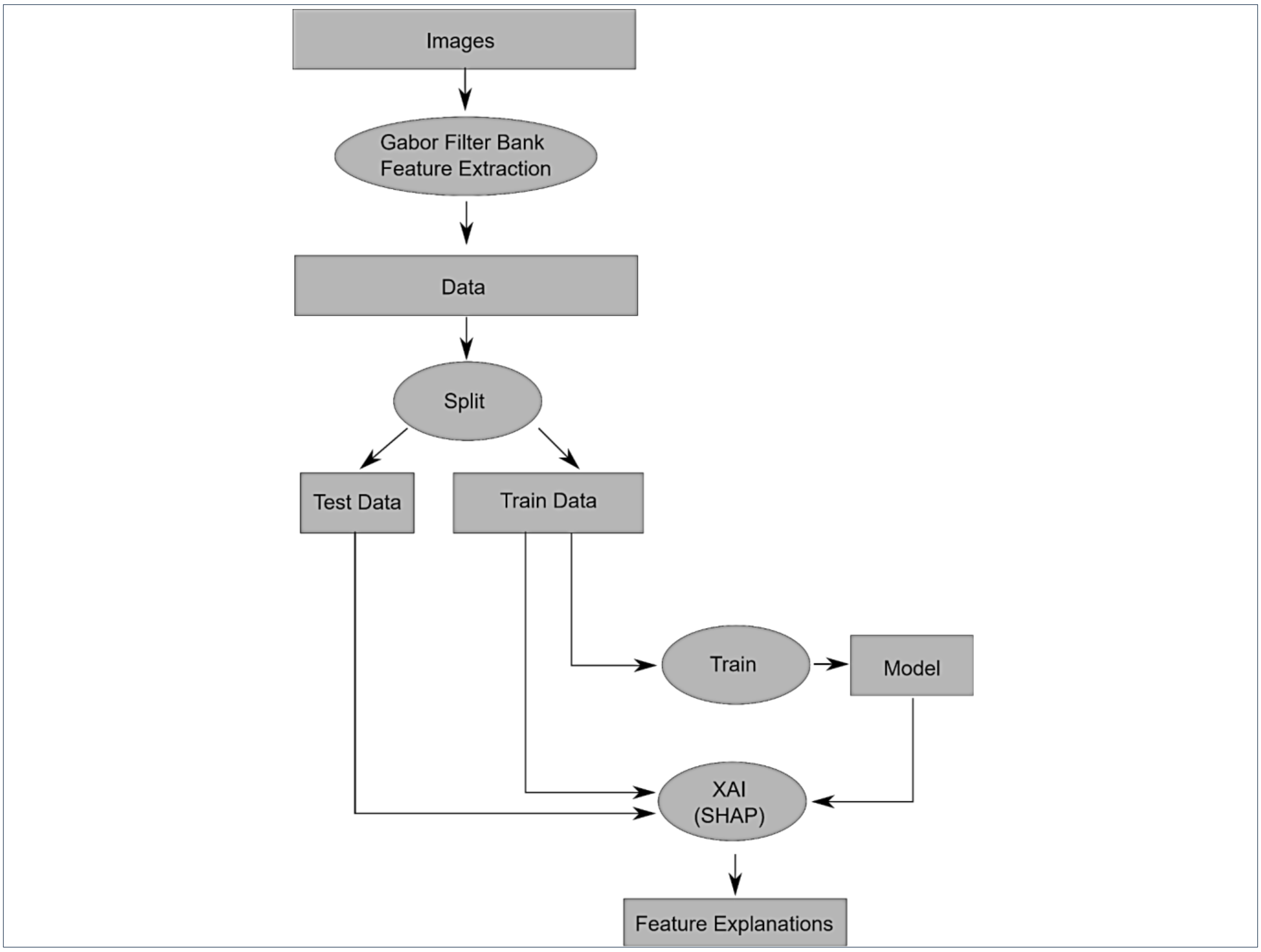

Fig. 4. General Method

3.1. Dataset and Preparation of Dataset

The images were captured using a high-resolution digital microscope to examine the samples that were manufactured through grinding, turning, and milling processes. The samples were carefully prepared and placed under the digital microscope to ensure accurate and detailed imaging of their surfaces. By capturing the images at a high magnification level, fine surface details, such as roughness, texture, and surface defects, were clearly visible and could be thoroughly analyzed.

The measurements were conducted under carefully controlled laboratory conditions. The nanometrology laboratory conditions were conditioned to ensure a stable and controlled environment throughout the measurement process. This conditioning involved maintaining consistent temperature, humidity, and lighting levels to minimize potential sources of variability and ensure accurate and reliable results. The measurement was realized under the same conditions for consistency and accuracy. By conducting the measurement under identical conditions, any potential variations or biases that could arise from changes in environmental factors, lighting, or other external influences are minimized. This approach ensures that the data collected is reliable and can be directly compared and analyzed without the confounding effects of different conditions. It also enhances the reproducibility of the results, allowing for meaningful comparisons and drawing valid conclusions based on the measurements obtained.

3.2. Feature Extraction using Gabor Filter Banks

Gabor Filter Bank (GFB) is a method commonly used in image processing for feature extraction (Guo et al., 2020; Hoang et al., 2020; Lee at al., 2017). It involves applying different types of filters on a local window. A 2D Gabor Filter consists of carrier and envelope parts as seen in (1). Carrier and envelope parts are given in (2) and (3), respectively. The carrier function is a two-dimensional sinusoid with wavelength λ and phase offset value φ. The Envelope Function is basically a circle equation, and the aspect ratio is adjusted by the variable γ. The x’ and y’ values are presented in (4) and (5), respectively, and the variable θ is orientation angle. By changing these parameters that make up a Gabor filter, many filter combinations can be created. These filters are convolved with each defined window on the image and converted to feature vectors.

$$g(x,y,\sigma,\theta,\lambda,\gamma,\varphi) = s(x,y,\theta,\sigma,\gamma) \times w_r(x,y,\theta,\lambda,\varphi) \tag{1}$$

$$wr(x,y,\theta,\lambda,\varphi) = e^{\left[-\frac{x\prime^2+\gamma^2 y\prime^2}{2\sigma^2}\right]} \tag{2}$$

$$s(x,y,\sigma,\gamma) = e^{\left[i(2\pi\frac{x\prime}{\lambda}+\varphi)\right]} \tag{3}$$

$$x' = x\,cos(\theta) + y\,sin(\theta) \tag{4}$$

$$y' = -x\,sin(\theta) + y\,cos(\theta) \tag{5}$$

Gabor filters (Teuner et al., 1995; Materka & Strzelecki, 1998; Riaz et al., 2013) are well-suited for texture analysis due to their ability to capture local frequency and orientation information. Gabor filter bank with varying scales and orientations to extract discriminative features from the metal surface images was constructed. Gabor filter banks were used to extract features with consistent parameters, including a window size of 31 pixels and a window stride of 15 pixels. The Gabor filter bank used theta (θ) values ranging from 0 to π in increments of π/8 in radians, sigma values of 1, 3, and 5, and frequency values of 0.1, 0.3, 0.5, 1, 3, and 5.

To extract features, the image obtained by convolution over each filter in the Gabor filter bank was analyzed for mean, variance, and peak-to-peak values. The extracted features provide valuable information about the surface texture, enabling effective differentiation and classification of the surfaces produced through grinding, milling, and turning.

In the extensive and thorough study, the tasks of image processing and feature extraction were performed using two prominent libraries, namely OpenCV and skimage. OpenCV, known for its robust computer vision capabilities, facilitated a wide range of image processing operations, including filtering, edge detection, and morphological transformations. On the other hand, skimage (scikit-image) library, well-known for its powerful image processing functions, provided various tools for feature extraction like texture analysis. The combined usage of these libraries contributed to the comprehensive and accurate analysis of images, enabling a deeper understanding of the underlying patterns and structures within the data.

3.3. Texture Detection with Machine Learning

The texture detection process involves utilizing a machine learning approach. To train and evaluate the model's performance, the dataset is split into two parts: a training set and a testing set. The dataset, derived from images through the Gabor filter bank method, is organized in a tabular format with 432 features (inputs) and 12328 samples. The division of the dataset into training and testing subsets is done in a stratified manner, ensuring that both sets maintain a representative distribution of the classes present in the data. Approximately 80% of the data is used for training, while the remaining 20% is reserved for testing the model's generalization abilities. The Random Forest Classifier algorithm is chosen for this texture detection task. It takes the 432 features as inputs and aims to predict the texture class, which represents the output in a multiclass classification setup. The training process involves learning the relationships between the input features and their corresponding output classes, while the testing process assesses the model's accuracy and performance on unseen data. By training and evaluating the Random Forest Classifier on this dataset, the machine learning approach enables the system to identify textures in new and unseen images with satisfactory accuracy and reliability. The sklearn library was also utilized for machine learning operations.

3.4. Explainable AI (XAI) with SHAP

The XAI process is a method used to explain the decisions of the machine learning model. The XAI process shows which features the model is classifying based on. This increases the reliability and intelligibility of the model. Different methods can be used for XAI processing, such as calculating the SHAP, ELI5 and LIME (Antoniadi et al., 2021; Bhattacharya, 2022).

In this chapter, the principles of XAI were implemented by applying to the SHAP library. The decision-making process of a machine learning model was understood, and insights were gained, making the model's predictions more transparent and interpretable. By utilizing SHAP values, the impact of individual features on the model's output was quantified, and their contributions towards specific predictions were discerned.

The SHAP library was employed for the XAI application with the aim of enhancing the trustworthiness and comprehensibility of the model, thereby facilitating informed decision-making in various practical domains. The SHAP value is a number that indicates how a feature affects the model's prediction. The SHAP value measures how far the feature deviates from the model's prediction from the expected value. The SHAP value shows both which features the model cares about in general and which features are effective in a single sample. To calculate the SHAP value, these steps are followed:

- create as many empty tables as the number of classes our model predicts. The number of rows of each table is equal to the number of samples in our dataset. The number of columns of each table is equal to the number of features in our dataset.
- For each sample in our dataset, it is determined what features are in that sample. Find models that have these features. These models are called submodels.
- For each submodel, find the class probabilities that that model predicts. Save these possibilities as a list.
- For each submodel, find how features that are not in that model change the model's prediction. For this, add or subtract that feature from the model and look at the difference in class probabilities the model predicts.
- For each submodel, average the amount of non-features that change the model's estimate. These values are the SHAP values of the features in that submodel.
- Sum the SHAP values across all submodels. Thus, for each instance, find the SHAP of each feature.
- Update the SHAP values tables. So, for each class, record the SHAP of each instance and each feature.

In this book chapter, the SHAP library is used to calculate the SHAP value for an output with 432 features and 3 classes in a multiclass classifier model trained using RF. Using the Tree Explainer class, the RF model was made compatible with SHAP. SHAP values were calculated for each feature in the data set. This method returns a matrix of SHAP values as the number of classes predicted by the model. The size of each matrix is equal to the number of samples and the number of features in your dataset (9863, 432).

4. Results and Discussion

4.1. Machine Learning Results: Metal Surface Texture Classification

A total of 9863 samples were used for training, and the Random Forest (RF) algorithm was applied to classify the data into 3 classes. The resulting confusion matrix for the training data is presented in Table 1, which shows an accuracy value of 1, indicating perfect classification performance. For the same model, a separate test was conducted using 2465 samples, and the corresponding confusion matrix is provided in Table 2. Remarkably, only one erroneous prediction was made during the test. In this case, the misclassified sample was originally from the milling (class 2) category but was incorrectly predicted as turning (class 3). These results demonstrate the high accuracy and robustness of the trained model, as it effectively classified most samples with minimal misclassification.

		Predicted			
		1	**2**	**3**	**∑**
Actual	**1**	3592	0	0	**3592**
	2	0	3591	0	**3591**
	3	0	0	2680	**2680**
	∑	**3592**	**3591**	**2680**	**9863**

Tab. 1. Test on train data results.

		Predicted			
		1	**2**	**3**	**∑**
Actual	**1**	897	0	0	**897**
	2	0	897	1	**898**
	3	0	0	670	**670**
	∑	**897**	**897**	**671**	**2465**

Tab. 2. Test on test data results.

4.2. Explainable AI (XAI) Results: Feature Importance with SHAP

In this chapter, the results of the research on XAI and feature importance analysis using SHAP are presented. The focus of the study was to enhance the interpretability of machine learning models by providing insights into the impact of individual features on the predictions. By using SHAP values, the influence of each feature in the model was quantified, revealing how it contributes towards or against the final prediction. Through the presentation of feature importance using SHAP, the aim was to shed light on the decision-making process of the model, making it more understandable for end-users.

The features annotated in red on the tape exhibit an increase in probabilities from the baseline probability towards a probability of 1.0, which corresponds to the prediction of the selected class (Figures 5-7). Conversely, the blue features exert an opposing effect, pushing the probabilities against the prediction of the selected class (Figures 5-7). The numerical values displayed on the tape represent the SHAP values associated with each feature, signifying the extent to which the feature and its corresponding value influence the probability either in favor of or against the selected class.

The application of XAI using SHAP not only improves the reliability and interpretability of machine learning models but also offers valuable insights that can lead to advancements in various practical domains, including metal surface texture classification and beyond.

Image number 1 represents a grinding texture image, while image number 2 is a milling texture image, and image number 3 is a turning texture image. The most influential features impacting their respective classifications are illustrated in Figure 5 for grinding, Figure 6 for milling, and Figure 7 for turning texture images.

The average value of the Gabor filter with a theta value of 0.79 radians (45°), sigma 5, and lambda value of 0.5, represents the most influential feature for all classes. The application of this filter on the three images (Image numbers 1, 2, and 3) and the resulting output is depicted in Figure 8.

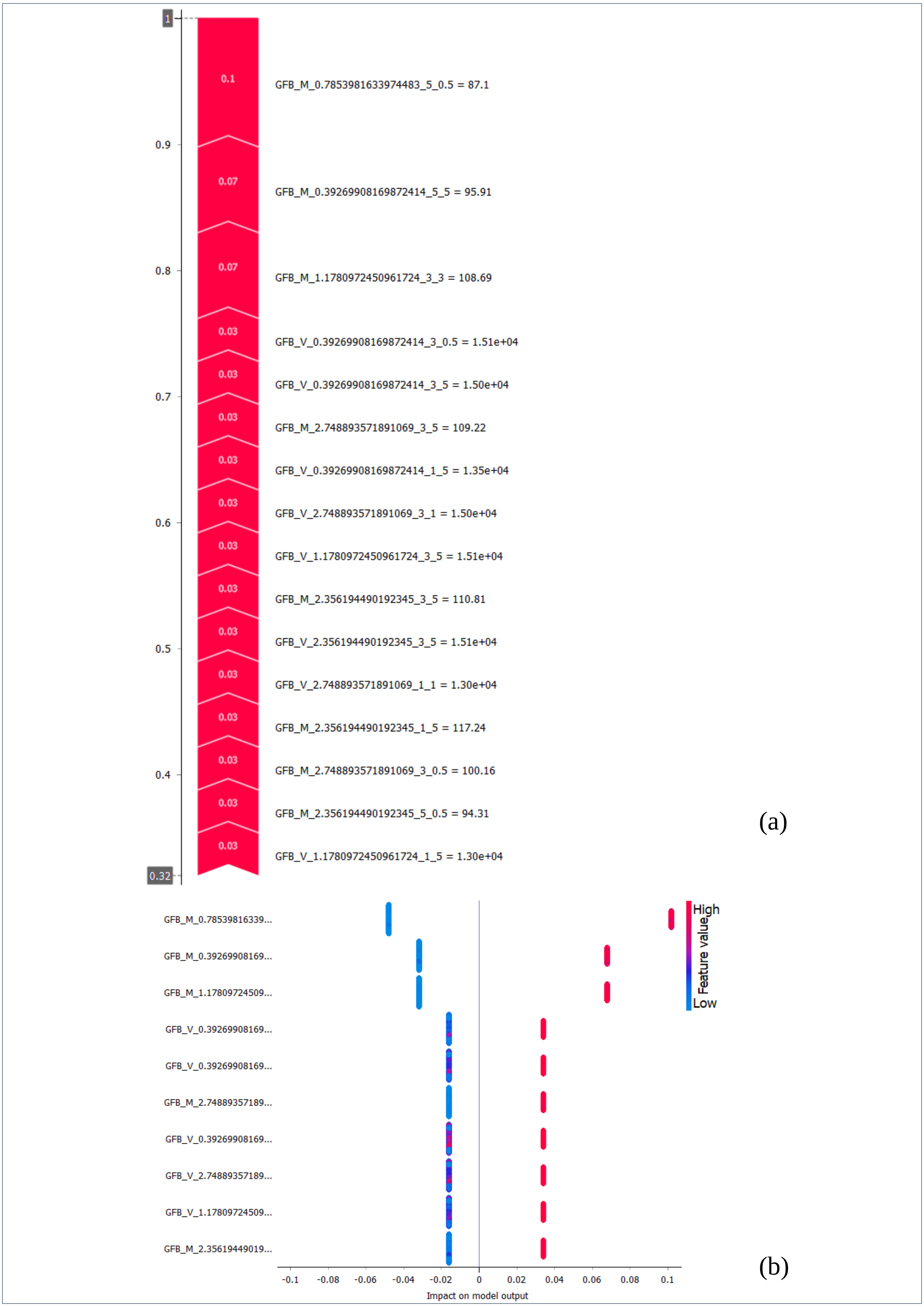

Fig. 5. Impact of Features on Classification Model (a) and SHAP values for Class 01 (b).

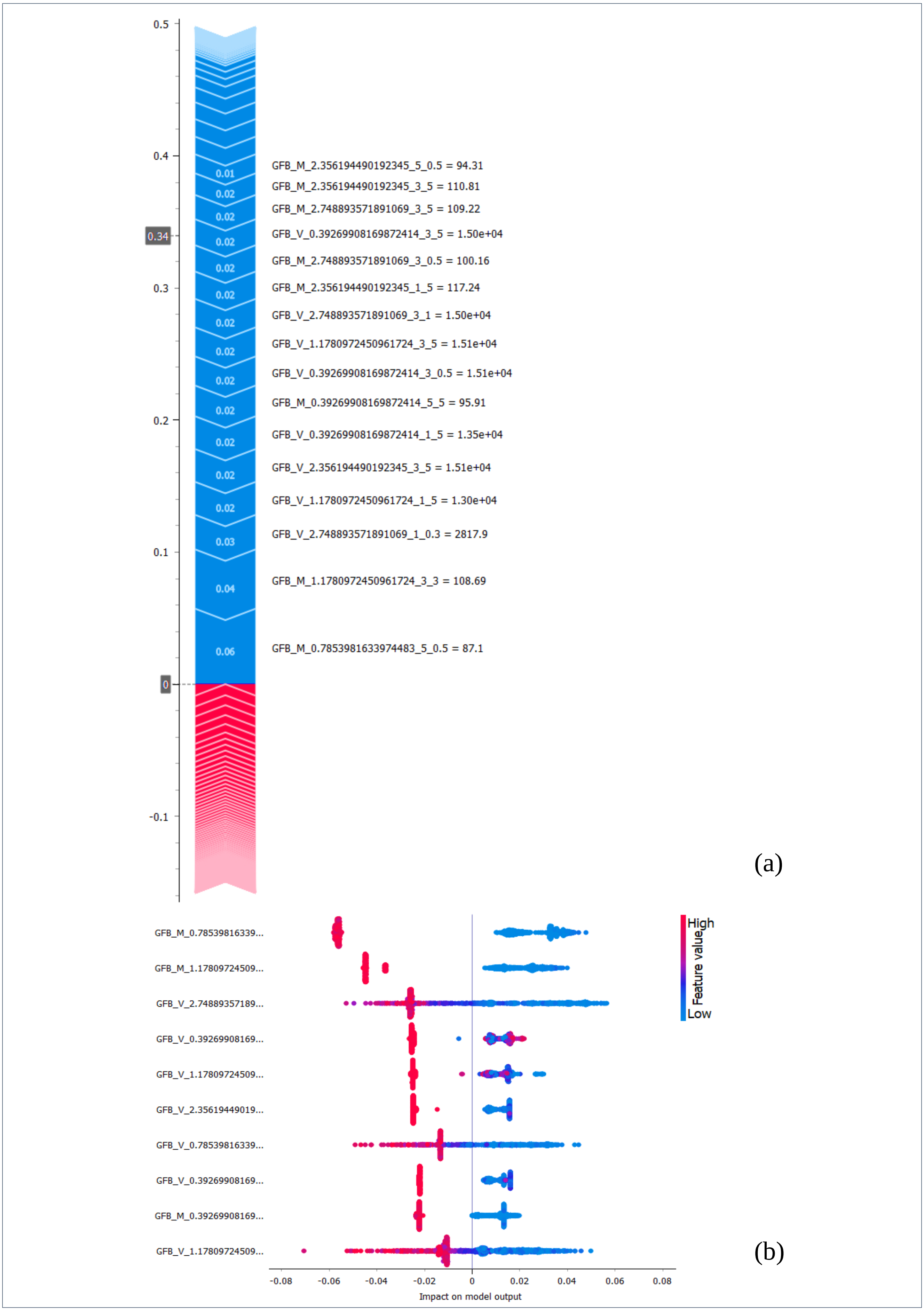

Fig. 6. Impact of Features on Classification Model (a) and SHAP values for Class 02 (b).

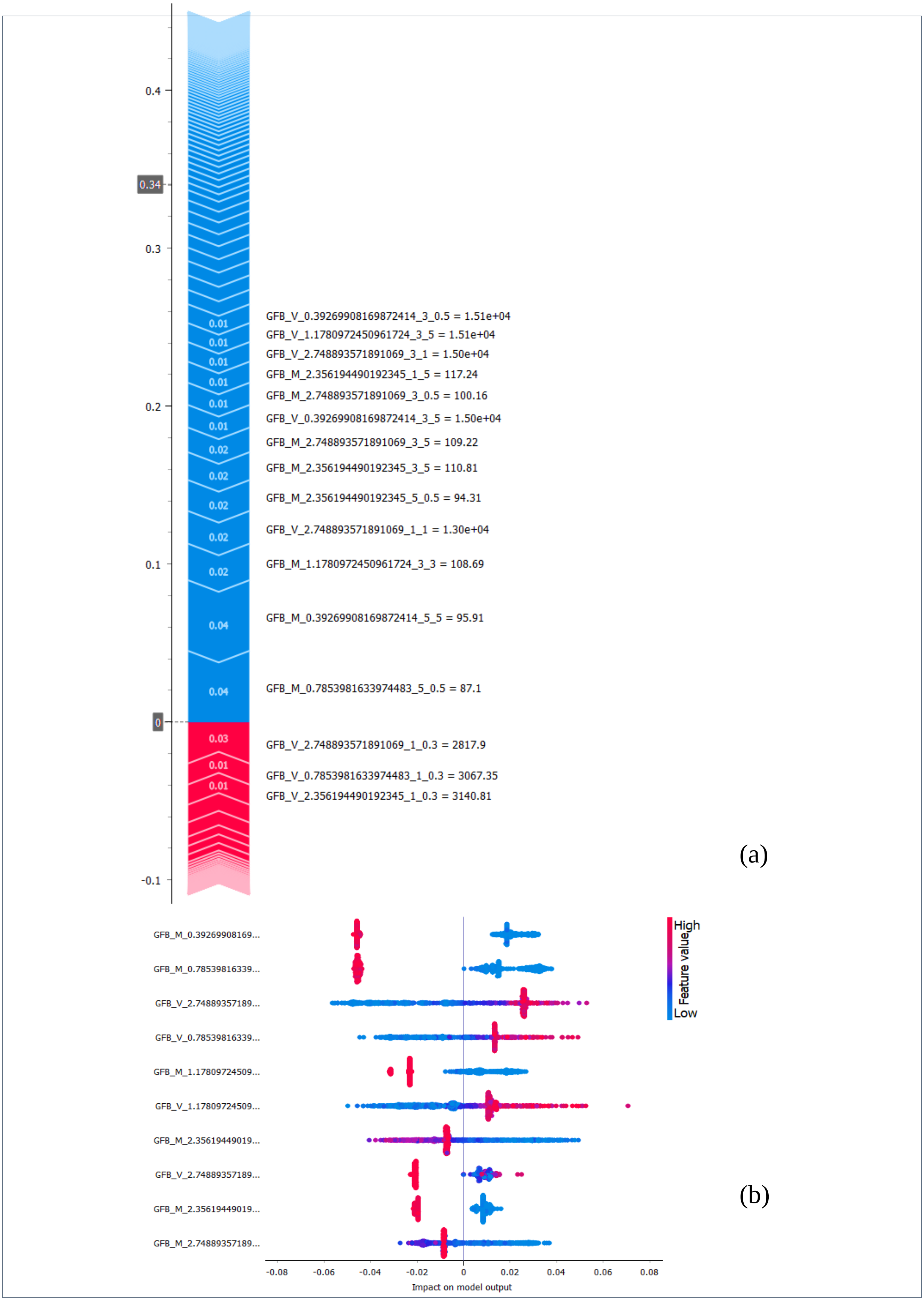

Fig. 7. Impact of Features on Classification Model (a) and SHAP values for Class 03 (b).

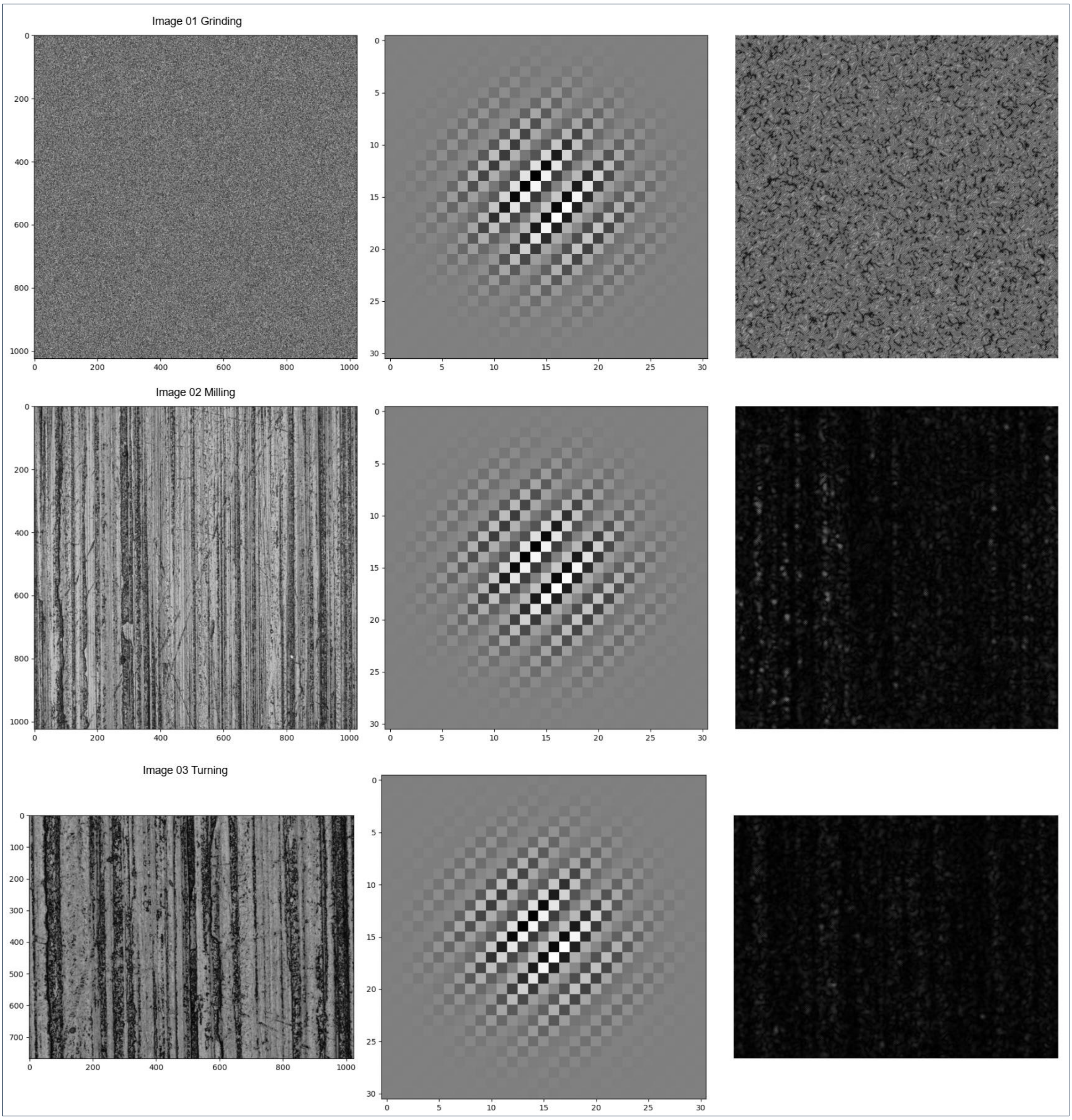

Fig. 8. Effect of most important feature (Gabor Filter Theta:45°, Sigma:5 and Lamda:0.5).

5. Conclusion

Metal surface texture classification is conducted using Gabor filter banks and XAI with SHAP. Texture features are extracted from metal surface images through the application of Gabor filter banks, capturing distinct spatial frequencies and orientations. The machine learning model is trained for texture classification based on the extracted Gabor filter responses. The model's decision-making process is made interpretable by incorporating XAI with SHAP, where the importance of each Gabor filter response is computed. High accuracy in classifying various metal surface textures is achieved through the proposed approach.

Insights for process optimization and quality control in industrial settings are facilitated by the interpretability offered by SHAP. The significance of interpretability in ensuring the reliability and applicability of AI-based systems in critical industrial domains is highlighted through this work.

In the extensive and thorough study, the tasks of image processing and feature extraction were performed using two prominent libraries, namely OpenCV and skimage. OpenCV, known for its robust computer vision capabilities, facilitated a wide range of image processing operations, including filtering, edge detection, and morphological transformations. On the other hand, skimage (scikit-image) library, well-known for its powerful image processing functions, provided various tools for feature extraction like texture analysis. The combined usage of these libraries contributed to the comprehensive and accurate analysis of images, enabling a deeper understanding of the underlying patterns and structures within the data. Machine learning operations were also conducted using the sklearn library in this chapter. Sklearn offers a user-friendly and consistent interface for a variety of machine learning tasks, including classification, regression, clustering, dimensionality reduction, and model selection.

In the analysis of this chapter, three texture images were utilized: image number 1 representing grinding, image number 2 for milling, and image number 3 depicting turning textures. The most influential features for their respective classifications were revealed through the examination of these images, as demonstrated in mentioned figures for different types of machining texture images.

The Gabor filter with a theta value of 0.79 radians (45°), sigma 5, and lambda value of 0.5 consistently emerged as the most influential feature across all classes. Its average value significantly influences the model's decision-making process, leading to robust predictions. To illustrate the impact of this crucial feature, the Gabor filter was applied to the three images (image numbers 1, 2, and 3), and the resulting output was observed. The application of the Gabor filter to the three texture images and the resulting observations offers valuable information that aids in informed decision-making and improves the model's transparency in real-world applications. This detailed analysis provides essential insights that contribute to the advancement of metal surface texture classification and other related domains.

The successful combination of Gabor filter banks and XAI with SHAP presents a promising direction for future research in texture classification and other related fields. As technology continues to evolve, the synergy between sophisticated feature extraction techniques and explainable AI will undoubtedly advance industrial processes and enrich our understanding of complex systems. Overall, this study contributes to the advancement of metal surface texture analysis and lays a foundation for building interpretable AI systems that cater to industrial needs while fostering transparency and accountability.

6. Acknowledgements

We sincerely thank Prof. Dr. Jan Torgersen, Chair of Materials Science and Head of the State Materials Testing Laboratory for Mechanical Engineering at TUM School of Engineering and Design, Technical University of Munich, for his invaluable support and guidance in shaping the outcome of this book chapter.

7. References

Aggarwal, A., Kumar, M. (2021). Image surface texture analysis and classification using deep learning. Multimedia Tools and Applications 80, pp. 1289-1309. https://doi.org/10.1007/s11042-020-09520-2.

Antoniadi, A.M., Du, Y., Guendouz, Y., Wei, L., Mazo, C., Becker, B.A., Mooney, C. (2021). Current Challenges and Future Opportunities for XAI in Machine Learning-Based Clinical Decision Support Systems: A Systematic Review. Applied Sciences 11, 11 (5088), pp. 1-23. https://doi.org/10.3390/app11115088.

Bhattacharya, A. (2022). Applied Machine Learning Explainability Techniques: Make ML models explainable and trustworthy for practical applications using LIME, SHAP, and more. Packt Publishing Ltd.

Bogrekci, I., Demircioglu, P. (2017). 3.18 Evaluation of Surface Finish Quality Using Computer Vision Techniques, Editor(s): MSJ Hashmi, Comprehensive Materials Finishing, Elsevier, 261-275. https://doi.org/10.1016/B978-0-12-803581-8.09180-3.

Cai, W., Deng, S., Liang, B., Xu, Q. (2010). Defect detection of bearing surfaces based on machine vision technique. International Conference on Computer Application and System Modeling. pp. 548-554. https://doi.org/10.1109/ICCASM.2010.5620311.

Chen, R., Huang, B., Liu, C., Yu, J., Yu, X. ve Zhou, Q. (2019). An Automatic Surface Defect Inspection System for Automobiles Using Machine Vision Methods. Sensors, 19(3), pp. 1-18. https://doi.org/10.3390/s19030644.

Demircioglu, P., Bogrekci, I., Durakbasa, N.M. (2013). Micro scale surface texture characterization of technical structures by computer vision. Measurement, 46(6), 2013, pp. 2022-2028. https://doi.org/10.1016/j.measurement.2013.02.012.

Gamage, P. & Xie, S.Q. (2008). A real-time vision system for defect inspection in cast extrusion manufacturing process. The International Journal of Advanced Manufacturing Technology 40, pp. 144-156. https://doi.org/10.1007/s00170-007-1326-z.

Guo, H., Li, B., Zhang, Y., Zhang, Y., Li, W., Qiao, F., Rong, X., Zhou, S. (2020). Gait Recognition Based on the Feature Extraction of Gabor Filter and Linear Discriminant Analysis and Improved Local Coupled Extreme Learning Machine, Mathematical Problems in Engineering. Vol. 2020, Article ID 5393058, pp. 1-9. https://doi.org/10.1155/2020/5393058.

Hoang, N. (2020). Image Processing-Based Spall Object Detection Using Gabor Filter, Texture Analysis, and Adaptive Moment Estimation (Adam) Optimized Logistic Regression Models. Advances in Civil Engineering. Vol. 2020, Article ID 8829715, pp. 1-16. https://doi.org/10.1155/2020/8829715.

ISO 4287:1997 Geometrical product specifications (GPS)-surface texture: profile method-terms, definitions and surface texture parameters. 2021.

ISO 8688-2:1989 Tool life testing in milling - Part 2: End milling. 2016

Jia, H., Murphey, Y. L., Shi, J., Chang, T.S. (2004). An intelligent real-time vision system for surface defect detection. IEEE. Vol. 3, pp. 239-242. https://doi.org/10.1109/ICPR.2004.1334512.

Lee, G.G., Huang, C.H., Chen, C.F., Wang, T.P. (2017). Complexity-Aware Gabor Filter Bank Architecture using Principal Component Analysis. Journal of Signal Processing Systems 89, pp. 431-444. https://doi.org/10.1007/s11265-017-1246-6.

Materka, A. & Strzelecki, M. (1998). Texture analysis methods-A review, Lodz Univ. Technol., Inst. Electron., Brussels, Belgium, COST B11 Report, pp. 9-11.

Neslihan, D., Eyinc, H., Demiricioglu, P., Bogrekci, I. & Durakbasa, N. (2022). Analysis of Correlation between Surface Roughness and Cutting Parameters in Different Machining Processes, Chapter 07 in DAAAM International Scientific Book 2022, pp.085-096, B. Katalinic (Ed.), Published by DAAAM International, ISBN 978-3-902734-34-1, Vienna, Austria. https://doi.org/10.2507/daaam.scibook.2022.07.

Sabry, E.S., Elagooz, S.S., El-Samie, F.E.A., El-Bahnasawy, N.A., El-Banby, G.M., Ramadan, R.A. (2023). Evaluation of feature extraction methods for different types of images. Journal of Optics 52, pp. 716-741. https://doi.org/10.1007/s12596-022-01024-6.

Shuai, Z., Xiaolin, D., Jing, Y., Yanni, H., Meng, C., Yuxin, W., Wei, Z. (2022). Comparison of different feature extraction methods for applicable automated ICD coding. BMC Medical Informatics and Decision Making 22. https://doi.org/10.1186/s12911-022-01753-5.

Seckin, A.C., Seckin, M. (2022). Detection of fabric defects with intertwined frame vector feature extraction. Alexandria Engineering Journal 61(4), pp. 2887-2898, https://doi.org/10.1016/j.aej.2021.08.017.

https://scikit-image.org/docs/stable/auto_examples/features_detection/plot_gabor.htm Accessed: 2023-07-01.

Pakdel, M. & Tajeripour, F. (2011). Texture classification using optimal Gabor filters. 1st International eConference on Computer and Knowledge Engineering (ICCKE), Mashhad, Iran. pp. 208-213, https://doi.org/10.1109/ICCKE.2011.6413352.

Riaz, F., Hassan, A., Rehman, S., Qamar, U. (2013). Texture classification using rotation- and scale-invariant Gabor texture features. IEEE Signal Processing Letters 20, pp. 607-610. https://doi.org/10.1109/LSP.2013.2259622.

Wang, M., Gao, L., Huang, X., Jiang, Y., Gao., X. (2019). A Texture Classification Approach Based on the Integrated Optimization for Parameters and Features of Gabor Filter via Hybrid Ant Lion Optimizer. Applied Sciences. 9(11):2173. https://doi.org/10.3390/app9112173.

Teolis, A. (1998). Continuous Wavelet and Gabor Transforms. In: Computational Signal Processing with Wavelets. Applied and Numerical Harmonic Analysis. Birkhäuser Boston. https://doi.org/10.1007/978-1-4612-4142-3_4.

Teuner A, Pichler O, Hosticka B.J. (1995). Unsupervised texture segmentation of images using tuned matched Gabor filters. IEEE Trans Image Process. 4(6), pp 863-70. https://doi.org/10.1109/83.388091.